2024 IEEE 63rd Conference on Decision and Control (CDC)
December 16-19, 2024. MiCo, Milan, Italy

Data-driven control for nonlinear automated vehicles with multi-description coding for handling data dropouts

Shuhua Zhang, Lifeng Ma, and Themistoklis Charalambous

Abstract— **This paper proposes a data-driven control (DDC) strategy for nonlinear automated vehicles, employing a multi-description coding (MDC) mechanism based on scalar quantization to address the challenges of data dropouts and limited bandwidth in networked communication environments. The developed MDC-based communication protocol enhances system robustness by reducing the probability of data dropout. It achieves this by transmitting multiple descriptions of source data through diverse channels, incorporating quantization and index reassignment to efficiently alleviate bandwidth constraints. Based on the reconstructed real-time data, a novel data-driven controller and a parameter estimation algorithm are designed, offering adaptability to varying driving conditions and rapid response in dynamic environments. A numerical simulation showcases the potential of the proposed approach as a reliable and efficient solution for the speed problem in nonlinear automated vehicles with challenging communication environments.**

Index Terms— **Nonlinear automated vehicles, data-driven control; multi-description coding mechanism, data dropouts, limited bandwidth.**

I. Introduction

Central to the field of automotive technology is the domain of speed control in automated vehicles, a factor influencing the safety and efficiency of autonomous transportation systems. Various strategies have been proposed to achieve optimal performance in terms of vehicle stability and energy efficiency [1], [2]. However, most of them are model-based control methods. For nonlinear automated vehicles, data-driven control (DDC) techniques [3], [4] have been explored, which dynamically adjust vehicle speed using real-time sensor data.

DDC schemes are proving to be highly effective in navigating the complex and fluctuating environments that are typical of autonomous driving, but their effectiveness is heavily reliant on the consistent availability of reliable real-time data from an array of sensors and navigation systems [5]. In practical scenarios, the integrity of these data streams is often compromised by challenges such as data dropouts or limited bandwidth in networked communication channels. Addressing these issues is becoming increasingly important, particularly in the context of nonlinear automated vehicles, where network limitations impact the control algorithms.

To address the challenges associated with network limitations, researchers have explored several strategies. Among these techniques, predictive control methods [6] and compensation-based cooperative model free adaptive iterative learning control methods [7] are commonly employed to mitigate the effects of data dropouts, while bandwidth limitations are often handled using quantization-based and event-based control techniques [8]. Despite these advances, the literature reveals a gap in comprehensive research addressing both data dropouts and bandwidth constraints simultaneously in automated vehicles. Recently, some studies have introduced quantified coding communication protocols [9], [10] to alleviate these network communication issues, showing promising results. However, the application of these studies to the specific speed control problems in complex nonlinear automated vehicle systems has not been studied before.

In response to the aforementioned gap, this paper proposes an innovative DDC approach for nonlinear automated vehicle systems, which features novel structural design and algorithm implementation. The developed control method integrates a multi-description coding (MDC) mechanism [9], [11] with scalar quantization, enabling multiple quantized data streams to be transmitted over independent network channels. This method of data transmission across multiple channels significantly reduces the probability of simultaneous data loss, thereby alleviating the issue of packet dropouts. Furthermore, considering that scalar quantizers can convert floating-point numbers into fixed-bit integers, substantially reducing data size, such quantized data can decrease the demand on network bandwidth without sacrificing excessive information. Thus, incorporating scalar quantization within the MDC framework is key to ensuring data integrity and efficient transmission, offering a robust solution to the complex speed control challenges in nonlinear automated vehicles. Moreover, the proposed MDC-based DDC approach uniquely operates without the need for explicit model information, relying completely on I/O data. This characteristic is advantageous in handling the complexities of nonlinear automated vehicle systems.

S. Zhang and L. Ma are with the School of Automation, Nanjing University of Science and Technology, Nanjing 210094, China (Emails: {zhangsh, malifeng}@njust.edu.cn).

T. Charalambous is with the Department of Electrical and Computer Engineering, School of Electrical Engineering, University of Cyprus, Nicosia, 1678, Cyprus (Email: charalambous.themistoklis@ucy.ac.cy). He is also a Visiting Professor with the Department of Electrical Engineering and Automation, School of Electrical Engineering, Aalto University, Espoo, Finland, and FinEst Centre for Smart Cities, Tallinn, Estonia.

The work of S. Zhang was supported in part by the National Natural Science Foundation of China under Grant 62273180, in part by the China Scholarship Council under Grant 202306840126, and in part by the Postgraduate Research & Practice Innovation Program of Jiangsu Province under Grant KYCX23_0477. The work of T. Charalambous was supported in part by the project MINERVA, which received funding from the European Research Council (ERC) under the European Union's Horizon 2022 research and innovation programme (Grant Agreement No. 101044629). Also, this work has been partly supported by the European Commission through the H2020 project FinEst Twins (Grant Agreement No. 856602).

II. Preliminaries and Problem Formulation

A. Preliminaries

$\mathbb{R}$, $\mathbb{Z}$, and $\mathbb{N}$ represent the sets of real, integers, and non-negative integers, respectively. $\mathbb{N}^+$ denotes the set of positive integers. $\mathbb{P}\{A\}$ means the occurrence probability of the event 'A'. $\mathbb{E}\{A\}$ stands for the expectation of event 'A' to occur. For $a \in \mathbb{Z}$ and $b \in \mathbb{N}^+$, $a = b\lfloor \frac{a}{b} \rfloor + \langle \frac{a}{b} \rangle$ is true, where $\lfloor \frac{a}{b} \rfloor$ and $\langle \frac{a}{b} \rangle$ are the quotient and rest obtained on dividing a by b, respectively. Include the symbol $\wedge$ which is the logical "AND", and $\vee$ is the logical "OR".

B. System Model

The following assumptions are made to simplify the system dynamics [12]:

Assumption 1: The tire longitudinal slip is considered negligible, and the powertrain dynamics are modeled as a first-order inertial transfer function.

Assumption 2: The vehicle is modeled as a rigid, symmetrical body, focusing primarily on primary dynamic responses.

Assumption 3: Interactions between pitch/yaw motions and longitudinal dynamics are disregarded to simplify the vehicle model.

Consider an automated vehicle system with the following nonlinear dynamics [13], [14]:

$$\dot{v} = \frac{1}{m}\left(\frac{\varpi}{R}T - C_A v^2 - mgl\right), \tag{1}$$

where $v \in \mathbb{R}$ represents the velocity of the vehicle; $T \in \mathbb{R}$ is the driving/braking torque; ϖ is the mechanical efficiency of driveline; m and R are the vehicle mass and the tire radius, respectively; C_A is the lumped aerodynamic drag coefficient; g is the acceleration due to gravity; l is the coefficient of rolling resistance. Let the sampling time as h, system (1) can be discretized as:

$$\begin{aligned} v(t+1) =& v(t) + \frac{h\varpi}{mR}T(t) - \frac{hC_A}{m}v^2(t) - hgl \\ =:& f(v(t), u(t)), \end{aligned} \tag{2}$$

where $u(t) := T(t)$ is the input; $f(\cdot)$ is a nonlinear function, and the partial derivative of $f(\cdot)$ with respect to input $u(t)$ as $\frac{\partial f(\cdot)}{\partial u(t)} = \frac{h\varpi}{mR}$, which means that the partial derivative with respect to $u(t)$ is continuous and bounded, and the control direction is fixed.

Assumption 4: System (2) satisfies the general Lipschitz condition, that is, the inequality $|\Delta v(t+1)| \leq b|\Delta u(t)|$ holds for $\Delta u(t) \neq 0$, where $\Delta v(t+1) \triangleq v(t+1) - v(t)$; $\Delta u(t) \triangleq u(t) - u(t-1)$; and $b > 0$ is a positive constant.

Remark 1: Assumption 4 is reasonable within practical scenarios as it reflects the physical and engineering limitations inherent in the rate of change of an automated vehicle's speed. For example, to mitigate the impacts of sudden or unpredictable changes on safety and comfort, the design of the control system must ensure that the speed changes remain within a predictable and controllable range under all operating conditions.

Lemma 1: Consider the nonlinear automated vehicle system (2) satisfying Assumption 4 and $\Delta u(t) \neq 0$. By resorting to the compact-form dynamic linearization method [15], system (2) can be described by the following dynamic linear data model:

$$v(t+1) = v(t) + \phi(t)\Delta u(t), \tag{3}$$

where $u(t)$ and $v(t)$ are the control input and system output, respectively; $\phi(t) = \frac{h\varpi}{mR} + \frac{\Delta v(t)}{\Delta u(t)}\left(1 - \frac{hC_A}{m}(v(t) + v(t-1))\right)$ represents the time-varying parameter satisfying $|\phi(t)| \leq b$. The parameter $\phi(t)$ captures all the complex dynamics of the nonlinear system and can be estimated online.

C. Problem Description

The main objective of this work is to design a DDC scheme to ensure the stability of the complex nonlinear automated vehicle system described in (2) with data dropouts and limited bandwidth. First, to mitigate the effects of packet dropouts caused by limited communication bandwidth, poor transmission network quality, and other factors, we propose a MDC transmission mechanism that reduces the probability of data loss through redundant channels. Building on this, the paper further develops a DDC algorithm to ensure the stability of the system.

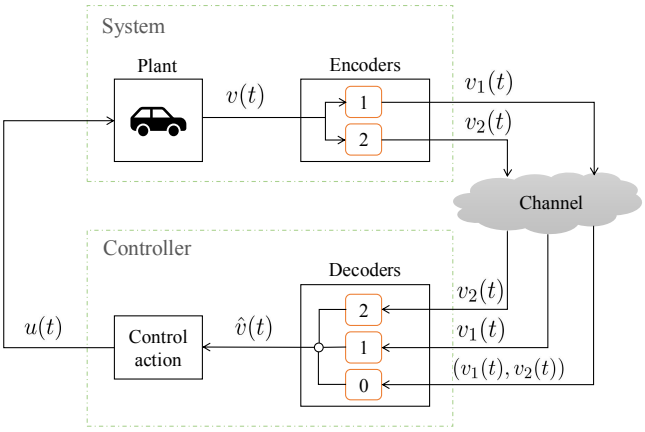

Fig. 1. Block diagram of MDC-based DDC method.

As shown in Fig. 1, the system output speed $v(t)$ is encoded into two descriptions, $v_1(t)$ and $v_2(t)$, which are transmitted through two independent channels and subsequently decoded to produce the data $\hat{v}(t)$ for controller design. The control input $u(t)$ is updated according to the designed control law to ensure that the system output $v(t+1)$ tracks the desired velocity v_d^*. Mathematically, the following condition should be satisfied:

$$\lim_{t\to\infty} |e(t+1)| \leq L, \tag{4}$$

where $e(t+1) = v_d^* - v(t+1)$ represents the speed error; L is a positive constant.

III. Main Results

A. Multiple Description Coding Communication Protocol

To enhance the robustness and reliability of the automated vehicle system, particularly in scenarios with data

dropouts, and to ensure effective and continuous operation in unstable network environments, this module proposes a MDC communication protocol. The main steps of the MDC mechanism, including the encoding and decoding processes, are outlined in detail below:

Encoding Process: The purpose of this process is to quantize the source $v(t)$ and utilize the following index assignment functions $\mathfrak{E}_1(\cdot)$ and $\mathfrak{E}_2(\cdot)$ to generate two descriptions $v_1(t) \in \mathbb{Z}$ and $v_2(t) \in \mathbb{Z}$, which are transmitted through two independent channels.

$$\begin{cases} v_1(t) = \mathfrak{E}_1\Big(Q\big(v(t)\big)\Big), \\ v_2(t) = \mathfrak{E}_2\Big(Q\big(v(t)\big)\Big), \end{cases} \tag{5}$$

where $v(t)$ is the input to the encoders; $v_1(t)$ and $v_2(t)$ are the output of the encoders 1 and 2, respectively; $Q\big(v(t)\big)$ is the scalar uniform quantizer, designed as

$$Q\big(v(t)\big) = \varrho(t),\ 2\big(\varrho(t)-1\big)\varsigma \le v(t) \le 2\varrho(t)\varsigma, \tag{6}$$

where $\varrho(t) \in \mathbb{Z}$ is the output of scalar uniform quantizer, and ς is the quantization density. Let the quotient $\kappa_1(t) = \lfloor \frac{\varrho(t)}{3} \rfloor$, and the remainder $\kappa_2(t) = \langle \frac{\varrho(t)}{3} \rangle$. The index assignment functions $\mathfrak{E}_1(\cdot)$ and $\mathfrak{E}_2(\cdot)$ are defined as

$$\mathfrak{E}_1(\cdot) = \begin{cases} \kappa_1(t), & \text{if } \kappa_2(t) = 0, \\ \kappa_1(t), & \text{if } \kappa_2(t) = 1 \wedge \kappa_1(t) \text{ even}, \\ \kappa_1(t)+1, & \text{if } \kappa_2(t) = 1 \wedge \kappa_1(t) \text{ odd}, \\ \kappa_1(t)+1, & \text{if } \kappa_2(t) = 2 \wedge \kappa_1(t) \text{ even}, \\ \kappa_1(t), & \text{if } \kappa_2(t) = 2 \wedge \kappa_1(t) \text{ odd}, \\ \kappa_1(t)-1, & \text{if } \kappa_2(t) = -1 \wedge \kappa_1(t) \text{ even}, \\ \kappa_1(t), & \text{if } \kappa_2(t) = -1 \wedge \kappa_1(t) \text{ odd}, \\ \kappa_1(t), & \text{if } \kappa_2(t) = -2 \wedge \kappa_1(t) \text{ even}, \\ \kappa_1(t)-1, & \text{if } \kappa_2(t) = -2 \wedge \kappa_1(t) \text{ odd}, \end{cases} \tag{7}$$

and

$$\mathfrak{E}_2(\cdot) = \begin{cases} \kappa_1(t), & \text{if } \kappa_2(t) = 0, \\ \kappa_1(t)+1, & \text{if } \kappa_2(t) = 1 \wedge \kappa_1(t) \text{ even}, \\ \kappa_1(t), & \text{if } \kappa_2(t) = 1 \wedge \kappa_1(t) \text{ odd}, \\ \kappa_1(t), & \text{if } \kappa_2(t) = 2 \wedge \kappa_1(t) \text{ even}, \\ \kappa_1(t)+1, & \text{if } \kappa_2(t) = 2 \wedge \kappa_1(t) \text{ odd}, \\ \kappa_1(t), & \text{if } \kappa_2(t) = -1 \wedge \kappa_1(t) \text{ even}, \\ \kappa_1(t)-1, & \text{if } \kappa_2(t) = -1 \wedge \kappa_1(t) \text{ odd}, \\ \kappa_1(t)-1, & \text{if } \kappa_2(t) = -2 \wedge \kappa_1(t) \text{ even}, \\ \kappa_1(t), & \text{if } \kappa_2(t) = -2 \wedge \kappa_1(t) \text{ odd}. \end{cases} \tag{8}$$

Decoding Process: Index $\varrho(t)$ is estimated based on the received data, and subsequently decoded using the estimated values $\hat{\varrho}(t)$ to obtain the decoded output $\hat{v}(t)$. Mathematically, this can be described as:

$$\hat{v}(t) = (2\hat{\varrho}(t) - 1)\varsigma, \tag{9}$$

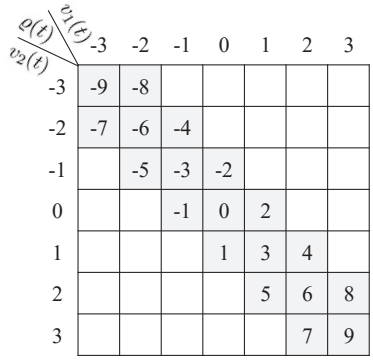

Fig. 2. Index assignment (The one-dimensional scalar quantized output $\varrho(t)$ is mapped using the index assignment functions $\mathfrak{E}_1(\cdot)$ and $\mathfrak{E}_2(\cdot)$, producing the coordinate pair $(v_1(t), v_2(t))$, which can be transmitted separately through two distinct channels).

where $\hat{\varrho}(t)$ is the estimated index of $\varrho(t)$, satisfying

$$\hat{\varrho}(t) = \begin{cases} z_0\big(v_1(t), v_2(t)\big), & \text{if } c_1(t) = 1 \wedge c_2(t) = 1, \\ z_1\big(v_1(t)\big), & \text{if } c_1(t) = 1 \wedge c_2(t) = 0, \\ z_2\big(v_2(t)\big), & \text{if } c_1(t) = 0 \wedge c_2(t) = 1, \\ \hat{\varrho}(t-1), & \text{if } c_1(t) = 0 \wedge c_2(t) = 0, \end{cases} \tag{10}$$

where $z_0(t)$, $z_1(t)$, and $z_2(t)$ are the central decoding function of decoder 0, and two side decoding functions of decoders 1 and 2, respectively, which are designed as

$$z_0(t) = \begin{cases} 3v_1(t), & \text{if } v_1(t) = v_2(t), \\ 3v_1(t)-1, & \text{if } v_1(t) = v_2(t)+1 \wedge v_2(t) \text{ even}, \\ 3v_1(t)-2, & \text{if } v_1(t) = v_2(t)+1 \wedge v_2(t) \text{ odd}, \\ 3v_1(t)+2, & \text{if } v_1(t) = v_2(t)-1 \wedge v_2(t) \text{ even}, \\ 3v_1(t)+1, & \text{if } v_1(t) = v_2(t)-1 \wedge v_2(t) \text{ odd}, \end{cases}$$

$$z_1(t) = 3v_1(t),$$

$$z_2(t) = 3v_2(t),$$

and $c_i(t), (i = 1, 2)$ are stochastic variables satisfying Bernoulli distribution

$$\begin{aligned} \mathbb{P}\{c_i(t) = 0\} &= \bar{c}_i, \\ \mathbb{P}\{c_i(t) = 1\} &= 1 - \bar{c}_i, \end{aligned} \tag{11}$$

where $c_i(t) = 1$ means the i-th channel works well; otherwise, data dropouts occur in the i-th channel; $\bar{c}_i \in [0, 1], i = 1, 2$ are known constants. Let

$$\alpha(t) = \begin{cases} 1, & \text{if } c_1(t) + c_2(t) \neq 0, \\ 0, & \text{if } c_1(t) + c_2(t) = 0. \end{cases} \tag{12}$$

The decoded output $\hat{v}(t)$ can be expressed as follows:

$$\hat{v}(t) = \begin{cases} v(t) - \tilde{v}(t), & \text{if } \alpha(t) = 1, \\ \hat{v}(t-1), & \text{if } \alpha(t) = 0, \end{cases} \tag{13}$$

where $\tilde{v}(t) = v(t) - \hat{v}(t)$ is the decoding error.

For $\alpha(t)=\alpha(t-1)=\cdots=\alpha(t-(\tau(t)-1))=0$ and $\alpha(t-\tau(t))=1$, we have

$$\hat{v}(t)=v\big(t-\tau(t)\big)-\tilde{v}\big(t-\tau(t)\big), \tag{14}$$

where $\tau(t)\in\mathbb{N}$, $\tau(t)\leq N<\infty$, and $N\in\mathbb{N}$. For simplicity of exposition, we omit the time argument and, hence, use τ instead of $\tau(t)$ hereafter. Hence, we have

$$\begin{aligned}&\mathbb{P}\left\{\sum_{j=0}^{\tau-1}\alpha(t-j)=0,\alpha(t-\tau)=1\right\}\\ =&(\bar{c}_1\bar{c}_2)^{\tau}(1-\bar{c}_1\bar{c}_2),\end{aligned} \tag{15}$$

indicating that the decoded output at time t is dependent on the values at a previous time $t-\tau$, given a series of conditions is satisfied by the parameter $\alpha(t)$, i.e., $\sum_{j=0}^{\tau-1}\alpha(t-j)=0$, and $\alpha(t-\tau)=1$.

Remark 2: The use of Bernoulli distribution random sequences to model multipath data losses provides several advantages. Firstly, the Bernoulli model (11) is simple and computationally efficient, making it suitable for real-time applications. Secondly, it captures the stochastic nature of data losses, which is essential for accurately representing the random occurrences of packet dropouts in a networked control system. In addition, the primary assumption of this model is that the duration of simultaneous and continuous data loss in both channels is bounded, as specified in (14) and (15). This assumption is reasonable because, in many practical systems, the probability of prolonged simultaneous data loss across multiple independent channels is low.

Remark 3: According to (5) and (9), we know that the MDC approach splits data streams into multiple, independently encoded descriptions, each sent over different network channels. It allows the system to reconstruct the original data with minimal loss, even if some packets are lost, thereby increasing tolerance to network instabilities. Additionally, we can adjust the quantization density ς based on network conditions, ensuring critical information can be transmitted when bandwidth is limited. This communication mechanism optimizes data transmission for reliability, making it ideal for automated vehicle systems where consistent, accurate data communication is crucial for safety and efficiency.

B. Data-Driven Control Scheme

In this subsection, we develop a MDC-based DDC control scheme, enabling the automated vehicle with the capability to maintain desired speed levels even under suboptimal network transmission conditions. The control scheme is outlined as follows:

$$u(t)=u(t-1)+\frac{\rho}{\lambda+|\hat{\phi}(t)|}\big(v_d^*-\hat{v}(t)\big), \tag{16}$$

$$\begin{aligned}\hat{\phi}(t)=&\hat{\phi}(t-1)+\frac{\eta\Delta u(t-1)}{\mu+|\Delta u(t-1)|^2}\big(\Delta\hat{v}(t)\\ &-\hat{\phi}(t-1)\Delta u(t-1)\big),\end{aligned} \tag{17}$$

$$\begin{aligned}&\hat{\phi}(t)=\hat{\phi}(1),\ \text{if}\ \left|\hat{\phi}(t)\right|\leq\varepsilon\vee|\Delta u(t)|\leq\varepsilon\\ &\vee\operatorname{sign}\big(\hat{\phi}(t)\big)\neq\operatorname{sign}\big(\hat{\phi}(1)\big),\end{aligned} \tag{18}$$

where $\hat{\phi}(t)$ is the estimated value of $\phi(t)$ with the initial value of $\hat{\phi}(1)$; $0<\rho<2/(N+1)$ and $0<\eta<2$ are step-size coefficients; $\lambda>b$ and $\mu>0$ are weight coefficients, b is the upper bound of $|\phi(t)|$; $\varepsilon>0$ is a sufficiently small scalar; $\Delta\hat{v}(t)\triangleq\hat{v}(t)-\hat{v}(t-1)$.

Remark 4: The DDC scheme based on MDC primarily differs from traditional PID in its robust handling of data transmission under unstable network conditions. Traditional PID control schemes might not focus as intensely on these network-specific challenges, concentrating more on adapting to system dynamics using real-time data. Furthermore, unlike the control method in [9], which is based on an index function, controller (16) is founded on feedback principles and previously decoded data to compensate for simultaneous packet loss events.

IV. Stability Analysis

Before focusing on the stability analysis of the automated vehicle, we first present the following theorem.

Theorem 1: For the nonlinear automated vehicle (2), which satisfies the Assumption 4, under the developed MDC-based DDC scheme (16)–(18), the system is guaranteed to exhibit asymptotic stability. Specifically, the speed error $\lim_{t\to\infty}|e(t+1)|\leq L$, $L\geq 0$, holds for parameters values that satisfy the conditions $0<\rho<2/(N+1)$ and $\lambda\geq b$.

Proof: According to the definition of speed error $e(t)$ in (4), we have

$$\begin{aligned}e(t+1)=&v_d^*-v(t+1)=v_d^*-v(t)-\phi(t)\Delta u(t)\\ =&e(t)-\frac{\rho\phi(t)}{\lambda+|\hat{\phi}(t)|}\big(v_d^*-\hat{v}(t)\big)\\ =&e(t)-\Phi(t)\big(v_d^*-\hat{v}(t)\big),\end{aligned} \tag{19}$$

where $\Phi(t)=\frac{\rho\phi(t)}{\lambda+|\hat{\phi}(t)|}$.

For $\alpha(t)=1$, we have

$$\begin{aligned}e(t+1)=&e(t)-\Phi(t)\big(v_d^*-v(t)+\tilde{v}(t)\big)\\ =&\big(1-\Phi(t)\big)e(t)-\Phi(t)\tilde{v}(t).\end{aligned} \tag{20}$$

For $\alpha(t)=\alpha(t-1)=\cdots=\alpha(t-\tau+1)=0$, and $\alpha(t-\tau)=1$, that is $\hat{v}(t)=\cdots=\hat{v}(t-\tau)=v(t-\tau)-\tilde{v}(t-\tau)$, where $0<\tau\leq N$ is an integer. Then, one has

$$\begin{aligned}e(t+1)=&v_d^*-v(t)-\phi(t)\Delta u(t)\\ =&\big(1-(\Phi(t)+\Phi(t-1)+\cdots\\ &+\Phi(t-\tau))\big)e(t-\tau)-\big(\Phi(t)\\ &+\Phi(t-1)+\cdots\\ &+\Phi(t-\tau)\big)\tilde{v}(t-\tau).\end{aligned} \tag{21}$$

By integrating (20) and (21), it can be established that an integer τ exists within the range $0\leq\tau\leq N$, ensuring that the speed error can be expressed as

$$e(t+1)=(1-\Psi(t))e(t-\tau)-\Psi(t)\tilde{v}(t-\tau), \tag{22}$$

where $\Psi(t)=\Phi(t)+\Phi(t-1)+\cdots+\Phi(t-\tau)$; $t-N\leq t-\tau\leq t+1$ represents the latest time instant can receive data from channel 1 or 2.

Let $\lambda \geq b$, there must exist a constant $0 < M_1 < 1$ such that the following inequality holds:

$$0 < M_1 \leq \frac{\phi(t)}{\lambda + |\hat{\phi}(t)|} \leq \frac{b}{\lambda + |\hat{\phi}(t)|} \leq \frac{b}{\lambda + \varepsilon} < 1 \quad (23)$$

Choosing $0 < \rho < 2/(N+1)$, it is guaranteed that

$$1 - \Psi(t) \leq 1 - \rho(\tau+1)M_1 \leq 1 - \rho(N+1)M_1 = b_1, \quad (24)$$

where $0 < b_1 < 1$ is a positive constant.

According to (6)–(9), we know that the decoding error satisfies $|\tilde{v}(t)| \leq 5\varsigma$ for $\alpha(t) = 1$.

Taking norm on both sides of (22), we have

$$\begin{aligned} |e(t+1)| \leq & \left|\left(1 - \Psi(t)\right)\right| |e(t-\tau)| + |\Psi(t)||\tilde{v}(t-\tau)| \\ \leq & b_1 |e(t-\tau)| + \rho(N+1)M_1 5\varsigma \\ \leq & b_1^{\frac{t}{N+1}} |e(1)| + \frac{\rho(N+1)M_1 5\varsigma (1 - b_1^{\frac{t}{N+1}})}{1 - b_1}. \end{aligned} \quad (25)$$

Thus, we can easily acquire

$$\lim_{t \to \infty} |e(t+1)| \leq \frac{\rho(N+1)M_1 5\varsigma}{1 - b_1}. \quad (26)$$

The proof primarily addresses the time-invariant desired velocity. For the case where the desired velocity is time-varying, the speed error will be related to the bound of the desired velocity. ■

V. Simulation

This section provides a numerical simulation to validate the effectiveness of the proposed MDC-based DDC method.

The parameters of the automated vehicle system are listed in Table I [2], [16]. The sampling time $h = 1$, and the desired speed is given as

$$v_d^* = \begin{cases} 25, & t \leq 1000, \\ 15, & t > 1000. \end{cases} \quad (27)$$

TABLE I

Vehicle Parameters.

Parameter	m	ϖ	R	C_A	g	l
Value	1300	0.88	0.25	1.1	9.8	0.016
Unit	kg	-	m	$\mathrm{N \cdot s^2/m^2}$	$\mathrm{m/s^2}$	-

The control parameters are selected as $\mu = 1.5$, $\eta = 0.1$, $\rho = 0.2$, $\lambda = 2$. The initial conditions are set as $v(1) = 0$, $u(1) = 100$, $\hat{\phi}(1) = 0.5$. The simulation results of the control scheme designed in this paper are presented in Figs. 3–6. In specific, for $\bar{c}_1 = \bar{c}_2 = 0.2$, Fig. 3 illustrates the velocity tracking performance, Fig. 4 presents the estimation error of the index $\tilde{\varrho}(t) = \varrho(t) - \hat{\varrho}(t)$, and Fig. 5 shows the values of parameter $\alpha(t)$. A critical observation from Figs. 4–5 is that $\alpha(954) = 0$, leading to the conclusiton that the error $\tilde{\varrho}(954) = 3 > 2$. Furthermore, the probability $\mathbb{P}\{\alpha(t) = 0\} = 89/2000 = 0.0445$, which approximates the probability $\mathbb{P}\{c_1(t) = c_2(t) = 0\} = 0.04$, and is significantly lower than $\mathbb{P}\{c_1(t) = 0 \text{ (or } c_2(t) = 0)\} = 0.2$. This analysis verifies that the proposed MDC communication protocol can effectively reduce the packet loss probability while ensuring data transmission accuracy within a certain range. Fig. 6 depicts the system output when $\bar{c}_1 = 0.97$, $\bar{c}_2 = 0.4$. This is particularly insightful for showcasing the system performance amidst challenges of high data dropouts. These figures provide clear evidence of the tracking performance achieved by the proposed control method.

Additionally, to facilitate a more compresensive comparison, the traditional PID controller $u(t) = k_p(v^* - \hat{v}(t)) + k_i \sum_{i=0}^{t}(v^* - \hat{v}(i)) + k_d((v^* - \hat{v}(t)) - (v^* - \hat{v}(t-1)))$ is used, where $\hat{v}(t) = c_1(t)v(t) + (1 - c_1(t))\hat{v}(t-1)$, $k_p = 0.8$, $k_i = 0.1$, and $k_d = 0.01$. The results are shown as Figs. 3–6 and Tables II–III. Table II shows the sum of absolute error $E = \sum_{t=1}^{2000} |e(t)|$. When the data loss probability for both channels is 0.2, the sum of absolute error $E = 3032$ in this paper is lower than the $E = 3779$ of the PID algorithm. As the data loss probability increases, the control algorithm proposed in this paper continues to maintain good tracking performance. Table III represents the computer memory usage of the system output $v(600)$, which needs to be transmitted over the network. Within the X86 architecture, integer data types can be defined as 8 bits and floating-point values as 32 bits (single-precision). It is evident that integers occupy less memory. The results demonstrate that the developed MDC-based DDC scheme not only demonstrates relatively superior tracking performance and robustness in scenarios with data dropouts in the transmission channels but also effectively mitigates the issue of limited bandwidth.

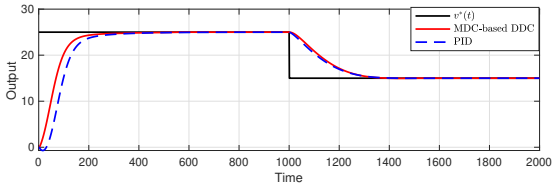

Fig. 3. System output (data loss probability $\bar{c}_1 = 0.2$, $\bar{c}_2 = 0.2$).

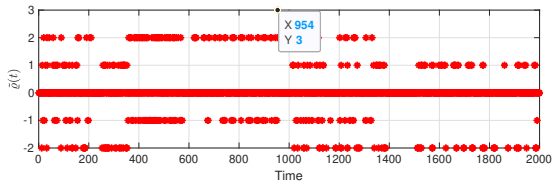

Fig. 4. The index estimation error $\tilde{\varrho}(t) = \varrho(t) - \hat{\varrho}(t)$ (data loss probability $\bar{c}_1 = 0.2$, $\bar{c}_2 = 0.2$).

TABLE II

Comparison of the Sum of Absolute Error

Data loss probability ($\bar{c}_1$ & $\bar{c}_2$)	0.2, 0.2	0.97, 0.4
This paper	3032	3157
PID	3779	4054

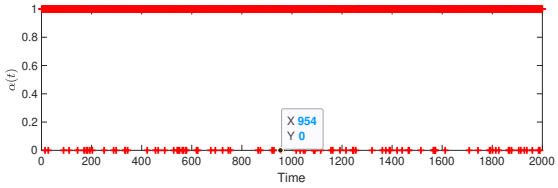

Fig. 5. Data loss moments on both channel 1 and channel 2. (if $\alpha(t) = 0 \Leftrightarrow c_1(t) + c_2(t) = 0$, it indicates data loss on both channels at time t).

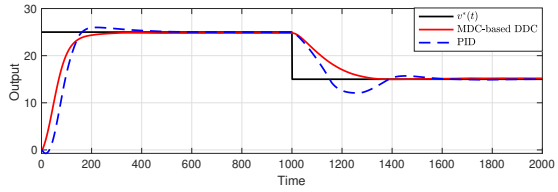

Fig. 6. System output (data loss probability $\bar{c}_1 = 0.97$, $\bar{c}_2 = 0.4$).

TABLE III

COMPARISON OF THE MEMORY CONSUMPTION

Algorithm	This paper	PID
$v(600)$	42	22.4421454928819
Binary	00101010	01000001101100111000100110000100
Bits	≥ 8	≥ 32

VI. Conclusions and Future Directions

A. Conclusions

This paper developed a MDC-based DDC scheme for nonlinear automated vehicles, specifically focusing on challenges posed by data dropouts and limited bandwidth in networked environments. The MDC communication protocol enhances automated vehicle system robustness by managing multiple data streams, ensuring reliable vehicle operation under challenging conditions. A data-driven controller and parameter estimation algorithm has been designed for precise speed control. The effectiveness of the developed control scheme is demonstrated through a numerical simulation.

B. Future Directions

To enhance the stability and reliability of automated vehicle systems, we will integrate advanced signal processing techniques and explore innovative methodologies in communication theory. This initiative aims to address complexities such as noise and time-delays, which significantly affect control system performance. Additionally, we will explore challenges associated with limited communication data rates within network communications.

References

[1] T. Fujioka and K. Suzuki, "Control of longitudinal and lateral platoon using sliding control," *Vehicle System Dynamics*, vol. 23, no. 1, pp. 647–664, 1994.

[2] Y. Zheng, S. E. Li, K. Li, F. Borrelli, and J. K. Hedrick, "Distributed model predictive control for heterogeneous vehicle platoons under unidirectional topologies," *IEEE Transactions on Control Systems Technology*, vol. 25, no. 3, pp. 899–910, 2017.

[3] Y. Zhang, L. Guo, B. Gao, T. Qu, and H. Chen, "Deterministic promotion reinforcement learning applied to longitudinal velocity control for automated vehicles," *IEEE Transactions on Vehicular Technology*, vol. 69, no. 1, pp. 338–348, 2020.

[4] Q. Wang, S. Jin, and Z. Hou, "Cooperative mfailc for multiple subway trains with actuator faults and actuator saturation," *IEEE Transactions on Vehicular Technology*, vol. 71, no. 8, pp. 8164–8174, 2022.

[5] Z. Hou, R. Chi, and H. Gao, "An overview of dynamic-linearization-based data-driven control and applications," *IEEE Transactions on Industrial Electronics*, vol. 64, no. 5, pp. 4076–4090, 2017.

[6] H. Wei, Y. Wang, J. Chen, and H. Zhang, "Resilient predictive control of constrained connected and automated vehicles under malicious attacks," in *IEEE International Conference on Industrial Cyber-Physical Systems (ICPS)*, 2023, pp. 1–6.

[7] Q. Wang, S. Jin, and Z. Hou, "Compensation-based cooperative mfailc for multiple subway trains under asynchronous data dropouts," *IEEE Transactions on Intelligent Transportation Systems*, vol. 23, no. 12, pp. 23 750–23 760, 2022.

[8] X. Bu, P. Zhu, Q. Yu, Z. Hou, and J. Liang, "Model-free adaptive control for a class of nonlinear systems with uniform quantizer," *International Journal of Robust and Nonlinear Control*, vol. 30, no. 16, pp. 6383–6398, 2020.

[9] S. Zhang, L. Ma, and X. Yi, "Data-driven control for nonlinear networked systems on basis of two description coding scheme," *IEEE Transactions on Automation Science and Engineering*, pp. 1–10, 2023.

[10] T. Li and L. Xie, "Distributed coordination of multi-agent systems with quantized-observer based encoding-decoding," *IEEE Transactions on Automatic Control*, vol. 57, no. 12, pp. 3023–3037, 2012.

[11] H.-T. Chan, C.-M. Fu, and C.-L. Huang, "A new error resilient video coding using matching pursuit and multiple description coding," *IEEE Transactions on Circuits and Systems for Video Technology*, vol. 15, no. 8, pp. 1047–1052, 2005.

[12] Y. Zheng, S. Eben Li, J. Wang, D. Cao, and K. Li, "Stability and scalability of homogeneous vehicular platoon: Study on the influence of information flow topologies," *IEEE Transactions on Intelligent Transportation Systems*, vol. 17, no. 1, pp. 14–26, 2016.

[13] M. Hu, X. Wang, Y. Bian, D. Cao, and H. Wang, "Disturbance observer-based cooperative control of vehicle platoons subject to mismatched disturbance," *IEEE Transactions on Intelligent Vehicles*, vol. 8, no. 4, pp. 2748–2758, 2023.

[14] Y. Bian, S. E. Li, W. Ren, J. Wang, K. Li, and H. X. Liu, "Cooperation of multiple connected vehicles at unsignalized intersections: Distributed observation, optimization, and control," *IEEE Transactions on Industrial Electronics*, vol. 67, no. 12, pp. 10 744–10 754, 2020.

[15] Z. Hou and S. Jin, *Model free adaptive control: theory and applications*. Boca Raton: CRC Press, 2013.

[16] J. Wang, S. E. Li, Y. Zheng, and X.-Y. Lu, "Longitudinal collision mitigation via coordinated braking of multiple vehicles using model predictive control," *Integrated Computer Aided Engineering*, vol. 22, no. 2, pp. 171–185, 2015.